International Journal of GEOMATE, Nov., 2023 Vol.25, Issue 111, pp.185-192
ISSN: 2186-2982 (P), 2186-2990 (O), Japan, DOI: https://doi.org/10.21660/2023.111.4014
Geotechnique, Construction Materials and Environment

NUMERICAL EVALUATION OF LOCAL RUBBER BEARINGS WITH VARIOUS CORE MATERIALS

Dimas Maulana Syirodjudin[1], *Tavio[1] and Bambang Piscesa[1]

[1]Department of Civil Engineering, Institut Teknologi Sepuluh Nopember (ITS), Surabaya, Indonesia

*Corresponding Author, Received: 07 July 2023, Revised: 19 Sep. 2023, Accepted: 24 Sep. 2023

ABSTRACT: Indonesia is a country that has a fairly high seismicity intensity. Therefore, Indonesia needs seismic protection. One of the earthquake protections is to use an isolator system. One type of isolator system that is widely available is LCRB (Lead Core Rubber Bearing). The long-term use of lead-lead in isolator cores can cause soil pollution, and the price of lead material is very expensive. Most rubber layers are obtained from the isolator's country of origin so researchers developed the use of local rubber originating from Indonesia. In this study, innovating isolator bearings using Indonesian local rubber with a core system on isolators that are filled using environmentally friendly materials and do not pollute the soil such as sand, resin, rubber, and HDPE named SCLRB (Sand Core Local Rubber Bearing), ECLRB (Epoxy Core Local Rubber Bearing), RCLRB (Rubber Core Local Rubber Bearing), and PCLRB (HDPE Core Local Rubber Bearing), The method carried out for the evaluation of core bearing performance using environmentally friendly materials is to use finite element simulation ABAQUS is used to evaluate bearing performance as well as mechanical behavior. The results of the simulation of elements to mechanical behavior found that the efficiency of the base isolator using local rubber and various core fillers is environmentally friendly, which provides considerable damping and stiffness improvements and effectively limits lateral displacement. The results of the element simulation analysis showed that the innovation of environmentally friendly materials sand, epoxy, rubber, and HDPE for isolator cores can replace lead in isolator cores that can pollute the soil.

Keywords: Abaqus,Base Isolation,Core Materials,Disaster Risk Reduction,Environmentally,Isolation System

1. INTRODUCTION

Indonesia is a country that has a fairly high seismic intensity. This is because three major plates pass Indonesia in the world, namely Eurasia, Indo-Australia, and the Pacific [1]. According to Pusgen data for 2018, Indonesia has experienced an increase in the number of active faults due to the activity of the Palu-Koro fault [2]. In 2018, a seismic event occurred due to the tectonic activity between these plates, resulting in a seismic event of magnitude 7.4 impacting the Palu region [3]. This earthquake caused tens of thousands of buildings to be damaged and collapse, as well as casualties due to falling buildings [4]. These conditions require Indonesia to have buildings that are resistant to strong earthquakes, which can reduce the risk of fatalities due to building collapses. Many methods have been developed and adopted by scientists to reduce the potential for damage to buildings due to earthquake activity, one of which is the use of base isolators as earthquake dampers [5,6]. The base isolator functions in the following way: a large earthquake will propagate to the isolation system before entering the main structure. Then, the isolation system dampens the existing seismic forces so that the vibration of the upper building is not too great [7,8]. Base isolator technology has become a mature energy dissipation technology in recent years. Laminated rubber bearing (LRB) is one of the most economical types of isolation systems in buildings for seismic energy dissipation purposes [9,10]. Research focuses on creating rubber bearings with shim layers made of fiber utilizing Indonesian natural rubber, with the goal of proving that carbon fiber and fiberglass shim layers provide the same hyperplastic qualities as plate shim layers were carried out [11]. LRB performance can be improved by adding a lead core, which was first introduced by Robinson in 1977. The resulting lead core rubber bearing (LCRB) exhibits significant shear and compression stiffness compared to LRB [12]. In addition, the use of lead produces a low pressure of 10 MPa and recrystallizes at room temperature, increasing the damping properties of the bearings and the elastomeric stiffness [13]. The use of lead in bearing technology has advantages as well as disadvantages. Lead contaminates the soil and can persist for centuries [14]. People living around these areas are at high risk of exposure to lead, and exposure to lead is always harmful to human health [15]. Ghrewati et al conducted a numerical analysis of the effect of replacing lead cores with rubber on the mechanical properties of lead rubber bearings. They found that the inserted rubber core increased the cushioning's damping, and this study agreed that the introduction of the rubber core reduced the stiffness of the elastomeric bearing [16]. Tan and Hejazi proposed a new elastomeric bearing with a

steel core and a filler system consisting of granular and polymer fillers as an improvement over the conventional elastomeric bearings. Researchers have found that the application of a steel core and filler increases the shear strength and energy dissipation of the bearing while reducing damping. The researchers said that the system with fully filled sand was the most profitable because the increase achieved was the highest, while the decrease in attenuation was not significant [17]. This research develops elastomer bearings by replacing rubber layers using local Indonesian rubber and develops new findings of new materials to replace the lead that are not friendly to the environment in isolator cores and filling systems consisting of sand, resin, rubber, and HDPE fillers. Modeling of mechanical properties of materials using ABAQUS finite element simulation, the proposed elastomer bearing performance is compared with the elastomer bearing performance using lead. So as to get the best material to replace the lead filling. In the discussion of the next sub-chapter discusses the comparison of simulation models with experimental models carried out by previous researchers. After the model is validated, it continues with the analysis of element simulations until the model is developed. Data on the mechanics, stress and deformation properties of the model are obtained. After all the models are obtained, the results are drawn to conclude whether environmentally friendly materials can replace lead that is less environmentally friendly.

2. RESEARCH SIGNIFICANCE

The main objective of this research is to develop a variety of rubber cushion core fillings, including Sand, Epoxy, Rubber, and HDPE materials, to identify suitable alternatives to substitute for lead materials, which can cause environmental problems. Examine the mechanical properties demonstrated by the individual filler core local rubber bearing models, starting with analyzing energy dissipation, effective stiffness, damping ratio, characteristic stiffness, and post-melting stiffness. To ensure the characteristic behavior of each model, variations of the core material can be used as a substitute for lead material. So this base isolator is designed to be environmentally friendly and easily accessible, making it suitable for application in various building structures.

3. MATERIALS AND METHODS

3.1 General

To start modeling research using the finite element method, the first stage is validating the ABAQUS numerical model against the experimental research model produced by Tan et al. [18]. Figures 1 and Figure 2 illustrate the geometric model of the base isolator model and the validation results between the finite element and experimental models. Numerical validation analysis Testing the LCRB model using ABAQUS will use vertical compression and lateral displacement tests. A compression test of 180000 N and a lateral design displacement (horizontal load) of 30 mm is defined as the displacement at the point of loading. Three sinusoidal cycles of displacement are applied laterally; the frequency is known to be 0.566 Hz or 0.349 rad/sec in circular frequency. The time required to complete one cycle is 18 seconds with three sinusoidal cycles, where the force-displacement relationship for the last cycle is used to obtain the elastomeric bearing characteristics.

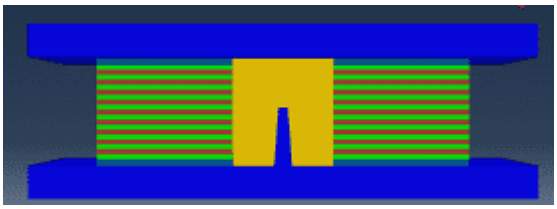

Fig.1 Sand core rubber bearing (SCRB)

3.2 Bearing Dimension

In the study shown in Figure 2, bearing dimensions in the development of isolator core filling systems, including SCLRB (Sand Core Local Rubber Bearing), ECLRB (Epoxy Core Local Rubber Bearing), RCLRB (Rubber Core Local Rubber Bearing), and PCLRB (HDPE Core Local Rubber Bearing), the proposed circular elastomeric bearing comprises a rubber layer (nr = 12) and a steel shim layer (ns = 11). The width and length of the top and bottom plates are (Wtop = Wbot = Ltop = 1294 mm), while the thickness of the plates is (Ttop = Tbot = 44 mm). Steel shim thickness (ts = 3 mm). The thickness of the rubber layer for the outermost layer (t_{ro} = 38 mm) with the number of layers is 2. The thickness of the inner rubber layer (t_{ri} = 36 mm) with the number of layers is 10. Bearing diameter (D_b = 1194 mm) and core diameter (D_{void} = 100 mm). Steel Core Dimensions (D_{ctop} = 20 mm, D_{cbot} = 30 mm, H_{cs} = 280 mm).

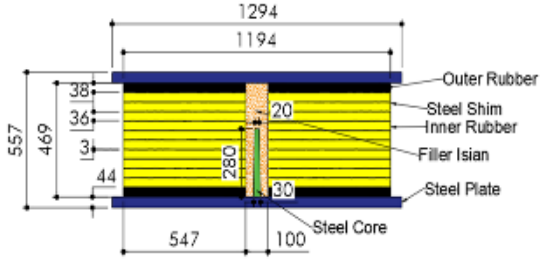

Fig.2 Dimension of the component in elastomeric

3.3 Material Properties

This section shows the mechanical properties of all the materials used in elastomeric bearing simulations by finite element modeling.

3.3.1 Rubber material

Bearing constituent material taken from the experimental results of Wijaya and Tavio [19] is Indonesian natural rubber, isoprene. The hardness of the proposed rubber is IRHD 60, and the corresponding shear modulus is 0.9 ± 0.15 N/mm2. Many hyperelastic models are available at ABAQUS [20]. Among the many hyperelastic models, Ogden's model is adopted in this study. The ability of the Ogden hyperelastic model to predict rubber behavior has proven reliable [21]. The strain function – energy *W* for Ogden's hyperelastic model is shown in Equation 1.

$$W=\sum_{i=1}^{N}\frac{2\mu_i}{\alpha_i^2}\left[\lambda_1^{\alpha_i}+\lambda_2^{\alpha_i}+\lambda_3^{\alpha_i}-3\right] \quad (1)$$

Where λ_1, λ_2, and λ_3 are principal strains. *N* is the order of the energy strain function. At the same time, μ_i and α_i are material constants, shown in Table 1.

Table 1 Material constants of Ogden hyperelastic model

Model Ogden N=3	
μ	α
0.3326	2.4466
0.3326	2.4466
0.3326	2.4466

Rubber hysteretic parameters using Bergstrom and Boyce method. The function of the hysteresis parameter is to evaluate the cyclic factor of the isolator. Rubber hysteretic parameters can be seen in Table 2.

Table 2 Hysteresis parameter defined for rubber material

S	$\hat{C}_1$	m	C_2
50	4 x 10-10	8	0

The parameters presented by Bergstrom and Boyce encompass the variables outlined in Table 2. In civil engineering, we denote the stress scaling factor as S, the creep factor as $\hat{C}1$, the effective stress exponent as m, and the creep strain as C_2. In this investigation, the cyclic shear examination yields a hysteresis curve, thereby facilitating the utilization of the Bergstrom and Boyce parameters to adapt the model to the empirical findings.

3.3.2 Material Steel, Sand, Epoxy, HDPE, and Lead

Table 3 shows the mechanical properties of steel, sand, epoxy, HDPE, and lead materials. Used in elastomeric bearing core simulation, the finite element modeling method.

Table 3 Mechanical properties of Steel, Sand, Epoxy, HDPE, and Lead

Material	Model	Properties
Steel	General elasticity [18]	E = 210 GPa
	General plasticity [18]	ν = 0.3
Sand	General elasticity [22]	E = 132 MPa
	General plasticity [22]	ν = 0.3
Epoxy	General elasticity [23]	E = 1317 MPa
	General plasticity [23]	ν = 0.35
		σ_y = 16.5 MPa
		ε_y = 1.16 %
		σ_u = 25.8 MPa
		ε_u = 2.9 %
HDPE	General elasticity [24]	E = 496.3 MPa
	General plasticity [24]	ν = 0.44
		σ_y = 26.1 MPa
Lead	General elasticity [18]	E = 18 MPa
	General plasticity [18]	ν = 0.3
		σ_y = 10 MPa

3.4 Model Meshing

Hexagonal elements unite all the components in one type of elastic pad. C3D8R elements, linear hexagonal solid elements reduced to eight nodes and three degrees of freedom under hourglass control, were used to model steel shims, steel cores, top and bottom plates, epoxy, HDPE, and lead. On the other hand, a C3D8RH element, a compact linear hexagonal solid element with eight nodes and three degrees of freedom under hourglass control and a constant pressure hybrid, is implemented for the rubber coating. A linear triangular prism with elements of six vertices and three degrees of freedom (C3D6) is constructed for the sand mass Figure 3.

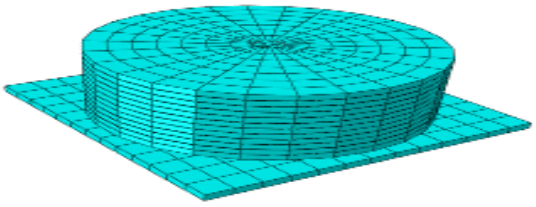

Fig.3 Meshing model for elastomeric bearings

3.5 Loading and Interaction

The proposed elastomeric bearings must have been tested to the requirements stipulated by SNI 1726-2019. Part of Article 12.8 of SNI 1726-2019 is used as a reference for testing elastomeric bearings [25]. Three full shear cycles are applied to the bearings in the fully engaged condition. In this study, the compressive design load was obtained from the results of the axial force-bearing reaction of the dead, live, and earthquake loads in the analysis of the Aster Inpatient Building, Tidar Hospital, six floors. With modifications to the core material variations SCLRB (sand core local rubber bearing), ECLRB (epoxy core local rubber bearing), RCLRB (rubber core local rubber bearing), and PCLRB (HDPE core local rubber bearing), the magnitude of the uniform vertical load is 2.75 MPa. All nodes on the top face are connected to the loading point via beam-type multi-point constraints, available in ABAQUS [20]. A lateral design displacement of 200 mm is applied as a cyclic lateral displacement at the loading point. Three sinusoidal cycles of horizontal displacement are defined and applied laterally, with a frequency of 0.1012 Hz, or 0.636 rad/s, in the circular frequency of Figure 4.

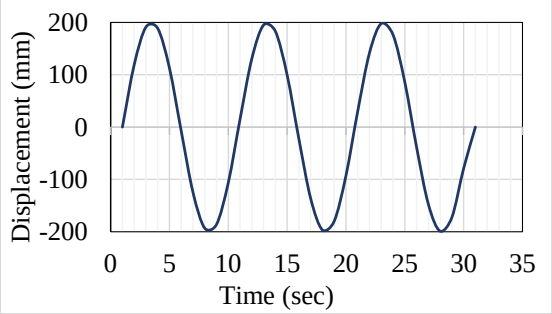

Fig.4 Sinusoidal lateral displacement cycles applied during finite element

Axial loads are applied in the first analysis step, while cyclic lateral displacements are applied in the second step. The axial load is distributed in the second stage, simulating the combination of axial load and lateral displacement during cyclic shear testing. The soffit on the bottom cover plate is expected to have an encastre boundary condition during analysis. As with the top plate, there is only translational motion along the x and z directions since shear and longitudinal forces are allowed, respectively. The top plate is held against rotation. This definition simulates the condition where the superstructure has very high rotational stiffness [18]. Tie constraints are defined for the contact interfaces between all bearing components.

3.6 Characteristic of Elastomeric Bearing

The characteristics of an isolation system are usually described in terms of the effective stiffness k_{eff}, the damping ratio ξ, the characteristic strength Q, and the post-melting stiffness kd. This parameter is derived from the lateral displacement force curve obtained from cyclic shear testing. The calculation method for this characteristic can be seen in equations 2, 3, 4, and 5 [18].

$$k_{eff} = \frac{F_p - F_n}{d_p - d_n} \tag{2}$$

$$\xi = \frac{2EDC}{\pi k_{eff}\left(d_p - d_n\right)^2} \tag{3}$$

$$Q = \frac{1}{2}\left(Q_p - Q_n\right) \tag{4}$$

$$k_d = \frac{1}{2}\left(\frac{F_p - Q_p}{d_p} - \frac{F_n - Q_n}{d_n}\right) \tag{5}$$

where d_p and d_n are the maximum positive and negative displacements applied during the test. F_p and F_n are the forces corresponding to d_p and d_n, respectively. EDC is the total energy dissipated in each cycle, determined by measuring the hysteresis loop area of the force-side displacement curves. Q_p and Q_n are the positive and negative intersections of the curve and the vertical axis.

4. RESULT AND DISCUSSION

4.1 Model Validation Result

After the numerical validation model has been modeled and finished running, the next step is to conduct a modeling analysis by comparing the validation results with experimental research to prove the accuracy of each model. The area of the hysteresis curve loop is a form of energy dissipation generated by the SCRB and ECRB models in damping lateral forces due to lateral loading, so the area of the hysteresis curve can be used to calculate the damping value. The following is a comparison plot of the hysteresis curve between the validation and experimental models, which can be seen in Figure 5 and Figure 6 from the study of Tan et al. [18].

The results of validating the SCRB and ECRB models with the experimental research model from Tan et al. [18] judging from the shape of the hysteresis curve in Figure 5 and Figure 6, there is a difference in the shape of the curve between the experimental control model and the validation model. In comparison, the FEA control curve model and the validation model are close to the same. The

difference occurs due to the imperfection of the model proposed by Bregstrom and Boyce in describing the rubber material in the elastomeric bearings tested.

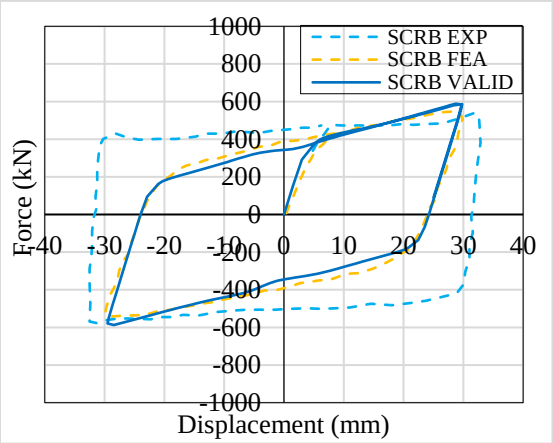

Fig.5 Hysteresis curve model validation SCRB

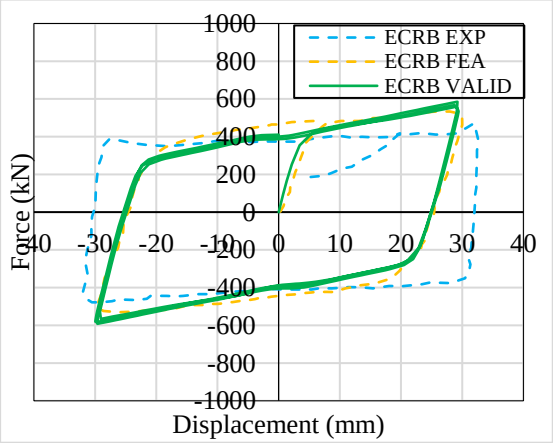

Fig.6 Hysteresis curve model validation ECRB

The inaccuracy of the experimental results of finite element analysis is caused by the mechanical properties of chloroprene rubber, where the unloading behavior is less dependent on time. As a result, the predicted hysteresis curve shows good agreement during the loading step.

The journal Tan et al [17] shows a significant discrepancy between the numerical model and the experimental results. The difference occurs due to the need for accuracy regarding implicit material variables and hyperelastic calibration values. As for the results of the validation analysis, the difference between the results of the numerical validation model and the results of the numerical control obtained is a difference that is still very representative or still acceptable. So that the modelling and numerical parameters can be used for the purposes of developing modified models.

4.2 Numerical Result Local Core Rubber Bearing with Material Variation

The following is the result of finite element analysis modeling for the development of the SCLRB (sand core local rubber bearing), ECLRB (epoxy core local rubber bearing), RCLRB (rubber core local rubber bearing), and PCLRB (HDPE core local rubber bearing) models, as well as using rubber local Indonesian for each layer of bearing pad. Evaluation of the development of isolator core material is useful for finding a replacement for copper lead plugs with environmentally friendly materials. The following is a hysteretic loop graph of the evaluation of material variations shown in Figure 7. Table 4 also shows the mechanical behavior of each model.

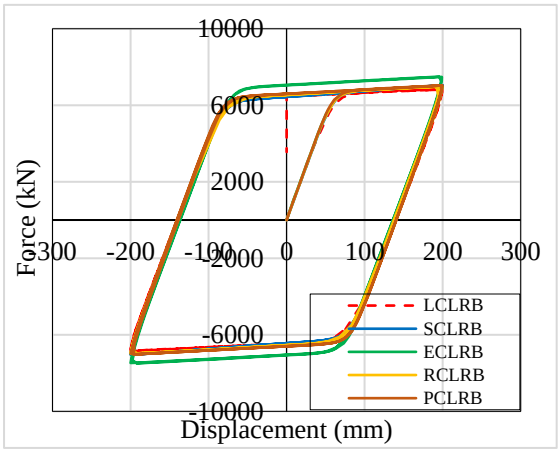

Fig.7 Result of hysteresis loops model core rubber bearing

The results of finite element numerical analysis, seen from the shape of the hysteresis curve in Figure 12 and observed from the area of the curve, show that the order of increasing energy dissipation ability occurs in the SCLRB (sand core local rubber bearing) model, ECLRB (epoxy core local rubber bearing), RCLRB (rubber core local rubber bearing), and PCLRB (HDPE core local rubber bearing), which is further improved compared to the LCLRB model. Based on the recapitulation of the results of the comparative analysis of mechanical characteristics in Table 4, the energy dissipation, stiffness, and damping ratio values for each variation of the rubber-bearing isolator core filler material proved that research on variations in core filling materials using sand, epoxy resin, rubber, and HDPE can be used as a substitute for environmentally friendly copper lead plugs.

Table 4 Comparison of core rubber bearing mechanical behavior characteristics with core material variations

Model	W_d (kNmm)	K_{eff} (kN/mm)	ξ (%)	Q (kN)	K_d (kN/mm)
LCLRB	3512399.84	34.36	40.88	6296.48	2.81
SCLRB	3525151.88	35.24	39.87	6439.20	3.02
Δ_{S-L} (%)	0.36%	2.56%	-2.46%	2.27%	7.74%
ECLRB	3774797.17	36.17	41.60	7052.62	0.88
Δ_{E-L} (%)	7.47%	5.26%	1.76%	12.01%	-68.52%
RCLRB	3608572.75	34.79	41.38	6542.51	2.05
Δ_{R-L} (%)	2.74%	1.26%	1.22%	3.91%	-27.12%
PCLRB	3657771.24	34.74	42.27	6599.14	1.61
Δ_{P-L} (%)	4.14%	1.12%	3.41%	4.81%	-42.77%

Judging from the type of material used to replace the isolator core, it is best to use materials that have shape memory alloy properties and hyperelastic properties because they have high flexibility so that they have energy dissipation values, considerable stiffness, and good damping values compared to other materials. Of the three epoxy, rubber, and HDPE materials, the good-shaped memory alloy material is HDPE. In terms of easy material maintenance, sand material is very superior because sand is a material in which sand is superior to the shear forces that occur where the mass of sand contributes to the shear strength by using friction between sand and sand particles, which also effectively transfers stress from the loading plate to the core. Steel because sand provides better rigidity but has less flexibility. Sand material is very useful in increasing the value of post-melting stiffness to control the displacement of the base isolator and superstructure.

4.3 Comparison of Stress Contours for Core Filling Material Variation

The effect of the variation of the core rubber bearing filling material is evaluated for its mechanical behavior and the maximum stress that occurs in the base isolator model. Below, Figures 8 to Figure 12, are the maximum stress for each base isolator model.

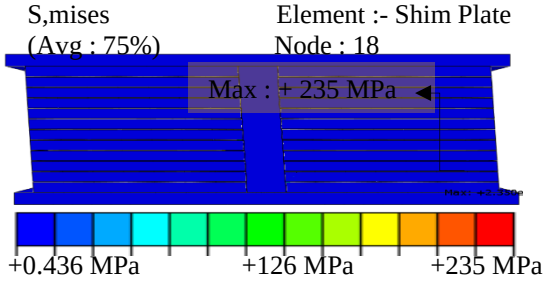

Fig.8 Maximum stress contour model LCLRB

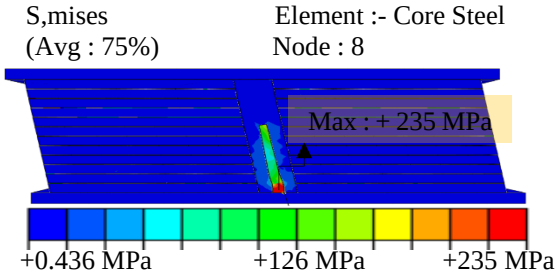

Fig.9 Maximum stress contour model SCLRB

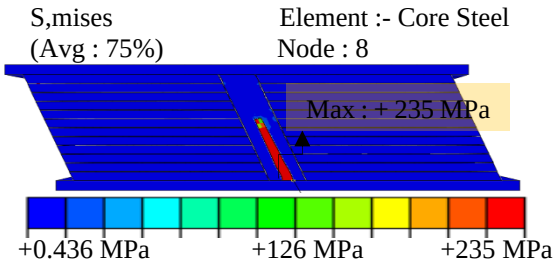

Fig.10 Maximum stress contour model ECLRB

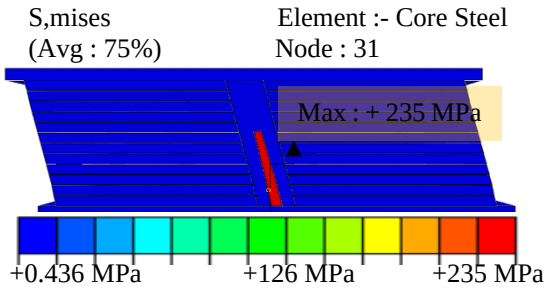

Fig.11 Maximum stress contour model RCLRB

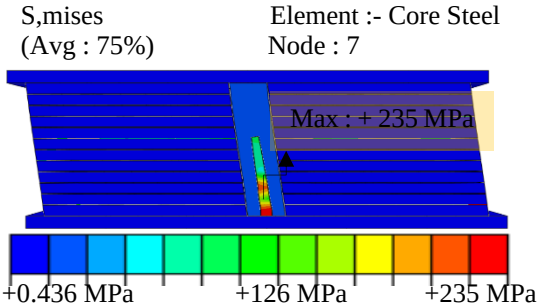

Fig.12 Maximum stress contour model PCLRB

The maximum stress experienced by the filler core rubber bearing is dependent on the material used to fill the isolator, which determines the maximum voltage value. In the LCRB test object, as shown in Figure 13, the lead stuffing layer experiences the highest stress at Shim steel layer 1, reaching a value of 235 MPa. The peak stress experienced within the shim region manifests at the periphery of the steel shim layer, resulting from the thermal effects induced by the friction between the rubber material and the compromised leads. In relation to the rubber layer, it is noteworthy that the maximum stress experienced remains consistently at a magnitude of 10.24 MPa. The stress concentration within the rubber layer is observed at the periphery of the aperture, resulting in detrimental effects on the rubber edge, primarily manifested as melting. The upper and lower steel plates endure the highest magnitude of stress at the periphery region, measuring 18.9 MPa. According to the theoretical framework proposed by Kelly and Neim, it is observed that lead exhibits a stress magnitude of 10 MPa. This stress is primarily attributed to alterations in the flow of stress, resulting in changes in the shape of the material. The maximum stress values observed in the material filling are attributed to different variations, specifically SCLRB, ECLRB, RCLRB, and PCLRB test objects depicted in Figure 9, Figure 10, Figure 11, and Figure 12. These test objects undergo maximum stress and yield in the steel core area, reaching a magnitude of 235 MPa. This stress is a result of the shear force experienced by the core steel due to the presence of the filler and isolator. Furthermore, the stress distribution from the top plate to the steel core leads to failure at the end of the steel core. The steel shims labeled as 1 and 11 are subjected to the highest stress, measuring 235 MPa. This is primarily due to the steel core system being in direct contact with both the top and bottom cover plates. Consequently, the steel shim encounters an equivalent maximum stress level as the steel core.

5. CONCLUSION

In this study, local rubber elastomeric bearings with a filling system consisting of sand, epoxy resin, rubber, and HDPE fillers can be drawn the following conclusions:

1. The results of the validation analysis of the numerical models of SCRB and ECRB in the experimental research of Tan et al. showed significant differences in the shape of the hysteresis curve in experimental with numerical due to the model proposed by Bregstrom and Boyce in describing rubber materials. However, it is still representative to be used as a reference for the development model.
2. The results of the mechanical behavior analysis of environmentally friendly core filler material models using local rubber include SCLRB, ECLRB, RCLRB, and PCLRB models. Good mechanical behavior is obtained from each model that can replace lead cores that are not environmentally friendly.
3. From the analysis of stress behavior it is known that the maximum stress in the local rubber cushion core filler model occurs in the steel core. Where the steel core occurs due to shear forces from the filler and isolator as well as the stress distribution from the top plate to the steel core.
4. The results of the element simulation analysis showed that the innovation of environmentally friendly materials sand, epoxy, rubber, and HDPE for isolator cores can replace lead in isolator cores that can pollute the soil.

6. ACKNOWLEDGMENTS

The authors gratefully acknowledge financial support from the Institut Teknologi Sepuluh Nopember for this work, under project scheme of the Publication Writing and IPR Incentive Program (PPHKI) 2023.

7. REFERENCES

[1] Wijaya U., Soegiarso R., Wijaya A., and Tavio., Numerical Study of Potential Indonesian Rubber for Elastomeric Base Isolators in Highly-Seismic Zones, Journal of Physics: Conference Series, Vol. 1477, 2020, pp. 1–7.

[2] Pusgen, Earthquake Source and Danger Map of Indonesia in 2017, 1st ed. Bandung: Research and Development Center for Housing and Settlements Research and Development Agency of the Ministry of Public Works and Public Housing, 2017, pp. 1-376

[3] Wu D., Ren Z., Liu J., and Guo P., Coseismic Surface Rupture During the 2018 Mw 7.5 Palu Earthquake, Sulawesi Island, Indonesia", GSA Bull., Vol. 133, 2021, pp. 1157–1166.

[4] Roosmawati N., Miller M.S., Cummins P.R. and Edwards M., Simulation of Scenario Seismic Ground Motion Using GMPEs: the 5 August 2018 Lombok Earthquake, West Nusa Tenggara, Indonesia, AEES 2022 National Conference, 2022, pp. 1–10.

[5] Habieb A.B., Milani G., Tavio, and Milani F., "Seismic Performance of a Masonry Building Isolated With Low-Cost Rubber Isolators, WIT

Trans. Built Environ, Vol. 172, 2017, pp. 71–82.
[6] Habieb A.B., Milani G., Tavio, and Milani F., Low Cost Frictional Seismic Base-Isolation of Residential New Masonry Buildings in Developing Countries: A Small Masonry House Case Study, Open Civil Engineering Journal, Vol. 11, 2017, pp. 1026–1035.
[7] Nguyen X.D., and Guizani L., Analytical And Numerical Investigation of Natural Rubber Bearings Incorporating U-Shaped Dampers Behaviour For Seismic Isolation, Engineerng Structure, Vol. 243, 2021, pp. 1-18.
[8] Mansour M.H., Hussein M.M., Akl A.Y., Assessment of Base-Isolated Buildings Designed Using International Damping Modification Factors, International Journal of GEOMATE, Vol. 21, No. 83, 2021, pp. 1–10.
[9] Habieb A.B., Milani G., Tavio, and Milani F., Low Cost Rubber Seismic Isolators For Masonry Housing In Developing Countries, AIP Conference Proceedings, Vol. 1906, 2017, pp. 1–4.
[10] Si M., Wu Y., Xu H., Li A., Xu Y., and Wang H., The Seismic Performance Evaluation Of Unbonded Laminated Rubber Bearings With End Rotation, Structures, Vol. 51, 2023, pp. 926–935.
[11] Rofiq H.I., Tavio, Iranata D., Model Validation of Carbon-Fiber and Glass-Fiber Reinforced Elastomeric Isolators Using Finite Element Method, IOP Conference Series: Earth and Environmental Science, Vol. 1116, No. 1, 2022, pp. 1-12.
[12] Robinson W.H., Tucker A.G., A Lead-Rubber Shear Damper, Bulletin of The New Zealand Society for Eartquake, Vol. 10, No. 3, 1977, pp. 151–153.
[13] Tavio, Sugihardjo H., Purniawan A., Lesmana Y., Behavior Of Rubber Base Isolator With Various Shape Factors, AIP Conference Proceedings, Vol. 1903, No. 1, 2017, pp. 1–10.
[14] Nagar M.C., Dotaniya M.L., Sharma A., Dotaniya C.K., Doutaniya R.K., and Saha J.K., Pressmud Overcome Lead Toxicity by Improving Spinach Biomass in Lead-Contaminated Soils, Enviromental Monitoring and Assesment, Vol. 195, No. 1, 2023, p. 107.
[15] Juberg D.R., Kleiman C.F., and Kwon S.C., Position Paper Of The American Council On Science And Health: Lead And Human Health, Ecotoxicol and Environtal Safety., Vol. 38, No. 3, 1997, pp. 162–180.
[16] Ghrewati B.E., Dada M., Alyosef I., and Jena T., Effect Of Replacing The Lead Core With Rubber on The Mechanical Properties of Lead Rubber Bearing, Materials Today Proceedings., Vol. 74, No. 1, 2023, pp. 627–635.
[17] Chun T.K., and Hejazi F., Rubber Bearing Isolator with Granular and Polymer Filler Core and Application on A Building, Structures, Vol. 42, 2022, pp. 309–332.
[18] Tan K.C., Hejazi F., Esfahani H.M., and Chong T., Development of Elastomeric Rubber Bearing Utilizing Core-and-Filler System, Structures, Vol. 37, 2022, pp. 125–139.
[19] Tavio, and Wijaya U., Experimental Study Of Indonesian Low-Cost Glass Fiber Reinforced Elastomeric Isolators (GFREI), *I*nternational Journal on Advanced Science Engineering Information Technology, Vol. 10, no. 1, 2020, pp. 311–317.
[20] Dessault Systemes., Abaqus Theory Guide Version 6.14, 2014.
[21] Wijaya U., Soegiarso R., and Tavio, Mechanical Properties of Indonesian Hyperelastic Low-Grade Rubber For Low-Cost Base Isolator, MATEC Web Conference, Vol. 276, 2019, pp. 1-7.
[22] Kamal Z.A., Arab M.G., and Dif A., Analysis Of The Arching Phenomenon of Bored Piles in Sand, Alexandria Engineering Journal, Vol. 55, No. 3, 2016, pp. 2639–2645.
[23] Li J., Tian C., Lu B., Xian Y., Wu R., Hu G., and Xia R., Deformation Behavior of Nanoporous Gold Based Composite in Compression: A Finite Element Analysis, Composite Structe, Vol. 211, 2019, pp. 229–235.
[24] Rueda F., Torres J.P., Machado M., Frontini P.M., and Otegui J.L., External Pressure Induced Buckling Collapse of High Density Polyethylene (HDPE) Liners: FEM Modeling And Predictions, Thin-Walled Structure, Vol. 96, 2015, pp. 56–63.
[25] BSN, Planning Procedures For The Seismic Resistance Of Buildings And Non-Building Structures (1726-2019), BSN, 2019, pp. 1–238.